



UKAEA-RACE-CP(25)01

Nikola Petkov, Ozan Tokatli, Kaiqiang Zhang, Huapeng Wu, Robert Skilton

A Kinematics Optimization Framework with Improved Computational Efficiency for TaskBased Optimum Design of Serial Manipulators in Cluttered Environments

This document is intended for publication in the open literature. It is made available on the understanding that it may not be further circulated and extracts or references may not be published prior to publication of the original when applicable, or without the consent of the UKAEA Publications Officer, Culham Science Centre, Building K1/0/83, Abingdon, Oxfordshire, OX14 3DB, UK.

Enquiries about copyright and reproduction should in the first instance be addressed to the UKAEA Publications Officer, Culham Science Centre, Building K1/0/83 Abingdon, Oxfordshire, OX14 3DB, UK. The United Kingdom Atomic Energy Authority is the copyright holder.

The contents of this document and all other UKAEA Preprints, Reports and Conference Papers are available to view online free at scientific-publications.ukaea.uk/

A Kinematics Optimization Framework with Improved Computational Efficiency for TaskBased Optimum Design of Serial Manipulators in Cluttered Environments

Nikola Petkov, Ozan Tokatli, Kaiqiang Zhang, Huapeng Wu, Robert Skilton

A Kinematics Optimization Framework with Improved Computational Efficiency for Task-Based Optimum Design of Serial Manipulators in Cluttered Environments

Nikola Petkov^{1,2}, Ozan Tokatli¹, Kaiqiang Zhang^{1,*}, Huapeng Wu², and Robert Skilton¹

Abstract—It is challenging to find optimum kinematic designs for non-standard robotic manipulators, e.g., medical, nuclear, and space manipulators, which are demanded to adapt to arbitrary complex tasks in constraints. Such design optimization can be modelled as a multi-dimensional non-convex optimization problem with nonlinear constrained conditions. However, it is non-trivial to ensure the essential reachability condition, i.e., the existence of continuous trajectories between demand positions for serial articulated manipulators, given complex spatial constraints, like obstacles and boundaries. Traditional solutions integrate standard motion planning or inverse kinematics algorithms within a kinematic-design optimization process, resulting in significant demand for time and computing resources. To accelerate design optimization at improved efficiency, we design a novel robust design framework built on a new kinematic design synthesis, which allows for simultaneously optimizing dimension and topology of a serial manipulator's kinematics for arbitrary tasks in constrained environments, using a generalised parametric kinematic model. Significantly, in contrast to standard solutions, we develop a novel computationally effective reachability verification method, which rapidly aborts infeasible motions by exploiting efficient collision checks, based on the Rapidly-exploring Random Tree (RRT) algorithm. The effectiveness of the proposed design framework is verified and evaluated by comparing to baseline benchmarks. Results demonstrate the novel design framework can accelerate kinematic design optimization by an order of magnitude compared to the current state-of-the-art, and optimise link dimension and joint type simultaneously of serial robots for cluttered environments.

Index Terms—Design Optimisaiton, Kinematics, Motion Planning, Reachability

I. Introduction

In applications such as medical [1], nuclear decommissioning [2], and in-space servicing [3], environmental constraints create collision hazard and limit target reachability. The development of customized, cost-efficient serial articulated robotic systems for cluttered environments requires reducing both the time spent on design and the associated hardware expenses. A key challenge in this process is to configure the manipulator's kinematics—irrespective of

*The work is funded by UKAEA/EPSRC Fusion Grant 2022/27 (EP/W006839/1) in the UK Atomic Energy Authority. The views and opinions expressed herein do not necessarily reflect those of the authority.

the degrees of freedom (DOFs)—while adhering to spatial limitations and design requirements (such as minimum link length) to successfully perform the tasks dictated by the robot's specific application [4]. Task based design [5], [6], uses prior knowledge of the task to optimise the robot kinematics. Patel et al. [7], gives a comprehensive review of the task based kinematic design problem, and offers a general methodology for task-based prototyping of serial robotic manipulators. More recently, Kivela et al. [8], and Maaroof et al. [9], provide another generic solution for gradient based kinematic design optimization evaluated on drilling robots, and medical application respectively. However, these studies assume collision free workspace where the inverse kinematics computation does not have any space constraints and is not hard to solve.

In cluttered environments, the use of motion planning is essential to assure the design requirements, particularly reachability, are met. Kahrs et al. [10], proposed an approach for kinematic design of medical robots called "RRT of RRTs" where the robot is designed by sampling both in the design space and the configuration of the robot. Baykal et al. [11], improves this approach by using Adaptive Simulated Annealing (ASA) [12] instead of RRT for sampling of the design space, and proves the approach is asymptotically optimal under mild assumptions. However, [11] does not provide a generic solution for the dimension-topology synthesis problem, i.e., optimizing the kinematic chain by exploiting variations in link length, joint actuation types, and kinematic-chain topology. Gamper et al. [13], proposes a pruning function objective, which minimises a maximal robot model by converging towards solutions with minimal number of links of the robot (by allowing link lengths to set to 0), instead of the minimal length of the robot, effectively reducing its DOFs (, i.e., optimizing the kinematic design by simplifying the kinematics complexity) in the process.

Despite these advances, there remains a lack of generic solution to task-based kinematic design optimization for serial manipulators, allowing to simultaneously optimize link dimension and kinematic topology while ensuring the reachability in heavily spatial constrained settings. Importantly, it is demanding to implement the optimization problem using a time efficient solution to the related reachability problem therein. This paper addresses these challenges and proposes a design framework which brings the following novelties to the optimal kinematic design problem.

1) An optimal design framework developed from a new

¹Nikola Petkov, Ozan Tokatli, Kaiqiang Zhang*(corresponding author) and Robert Skilton are with RACE, UKAEA, Culham, UK. {nikola.petkov, ozan.tokatli, kaiqiang.zhang, robert.skilton}@ukaea.uk

²Huapeng Wu is with the Department of Mechanical Engineering, Lappeenranta University of Technology, Lappeenranta, Finland huapeng.wu@lut.fi

kinematic design synthesis, which permit to search a complete solution space of a kinematic chain taking into account dimension (e.g., link length, joint range, etc.) and topology (e.g., joint actuation types and its topology in the kinematic chain) of serial robots tailored for constrained environments, using a generalised parametric kinematic model.

2) A novel extension to the Rapidly-exploring Random Tree (RRT) algorithm, that integrates trajectory collision detection to significantly enhance sampling efficiency.

Results of the comparative analysis of the proposed method for kinematic design optimization for reachability of targets in cluttered environments show significant improvement in rate of convergence over the baseline benchmarks [11] when using the proposed motion planning enhancement. The increased sampling efficiency of RRT, enables exploration of larger collision-free distances between nodes (way-points), significantly reducing motion planning time. Results of the evaluation of the proposed optimal design framework in 3D, show a time effective convergence towards optimal values of the design variables, minimising the: lengths and number of links, and ranges, number, and type (rotation or prismatic) of DOFs.

The paper is organized as follows. In Section II the formulation of the robot kinematic model, workspace, obstacles, trajectories and reachability of points in the work space are defined. Section III defines the optimization problem, i.e., the kinematic design synthesis. Section IV presents the effectiveness and advancement of the proposed approach via a case study. Discussions and conclusions are in Section V and Section VI, respectively.

II. PROBLEM STATEMENT AND FORMULATION

A. Robot Kinematic Model

The forward kinematics of a robot can be represented by the product of homogeneous transformation matrices which encode the geometry and actuation related components of the kinematic chain into a matrix notation. In the standard Denavitt-Hartenberg (DH) notation, the geometric parameters of the kinematic chain, which are α and a, are embedded together with the actuation variables of the robot θ and d.

In this work we are separating geometric parameters and actuation variables into separate transformation matrices and, initially, consider a 6 DOF actuation for each link: 3 rotations (ϕ, γ, ψ) and 3 translations (x, y, z). This provides the most general form of a serial kinematic chain and also allow us to perform search on the geometry of the robot without the meddling of the actuation variables. The generic forward kinematics model of the robot, from base frame to endeffector frame, used in this study is given by Eq. (1).

$$T_1^n = \prod_{i=1} T_i \cdot T_{\text{act},i} \tag{1}$$

where T_i is the geometric variables of the robot with constant DH values $(\alpha_i, a_i, \theta_i, d_i)$. Note that the θ and d in T_i are not actuation variables as in standard DH notation but they are only defining the geometry of the linkage at its initial

configuration and they are set to zero. On the other hand, $T_{\text{act},i}$ defines the contribution of the actuators into the forward kinematics. In the general case each joint is considered to be actuated with a 6 DOF actuator which leads to Eq. (2).

$$T_{\text{act},i} = \begin{bmatrix} R_x(\phi_i) & \mathbf{0} \\ \mathbf{0}^T & 1 \end{bmatrix} \begin{bmatrix} R_y(\gamma_i) & \mathbf{0} \\ \mathbf{0}^T & 1 \end{bmatrix}$$

$$\begin{bmatrix} R_z(\psi_i) & \mathbf{0} \\ \mathbf{0}^T & 1 \end{bmatrix} \begin{bmatrix} \mathbf{I} & \begin{bmatrix} x_i \\ y_i \\ z_i \end{bmatrix} \\ \mathbf{0}^T & 1 \end{bmatrix}$$
(2)

In Eq. (2), $R_x(\phi_i)$, $R_y(\gamma_i)$, and $R_z(\psi_i)$ are the rotation matrices corresponding to the Tait–Bryan angles ϕ_i , γ_i , $\psi_i \in \mathbb{R}$, and x_i , y_i , and $z_i \in \mathbb{R}$ are the translations in the local frame. The identity matrix $\mathbf{I} \in \mathbb{R}^{3\times 3}$ and the zero vector $\mathbf{0} \in \mathbb{R}^3$ are used to construct the homogeneous transformation matrix [14].

B. Workspace

We define the workspace W as a set of sphere obstacles and task points in 3D space.

Let O_k be the k^{th} sphere obstacle where $\mathbf{o}_k = (x_k, y_k, z_k) \in \mathbb{R}^3$ is the center of the k^{th} obstacle. $r_k \in \mathbb{R}$ is the radius of the k^{th} obstacle. Let m be the total number of obstacles. The set of obstacles \mathcal{O} is defined as

$$\mathcal{O} = \{ (\mathbf{o}_k, r_k) \mid \mathbf{o}_k \in \mathbb{R}^3, r_k \in \mathbb{R},$$

$$\forall k \in \{1, 2, \dots, m\} \}$$
(3)

Let $\mathbf{p}_j = (x_j, y_j, z_j) \in \mathbb{R}^3$ be the j^{th} task point. Let l be the total number of task points. The set of all task points \mathcal{P} is defined as

$$\mathcal{P} = \{ \mathbf{p} \mid \mathbf{p} \in \mathbb{R}^3 \text{ and } \|\mathbf{p} - \mathbf{o}_k\| > r_k, \}$$

$$\forall k \in \{1, \dots, m\}$$
(4)

We constrain the set of task points \mathcal{P} so that the task points are outside of the obstacles' radius (reachable).

The workspace W can be defined as the union of the set of obstacles and the set of task points:

$$W = \mathcal{O} \cup \mathcal{P} \tag{5}$$

C. Colliders

Let $\mathbf{c}_{i,\ell}=(x_{i,\ell},y_{i,\ell},z_{i,\ell})\in\mathbb{R}^3$ be the ℓ^{th} collider point along the i^{th} link of the robot, where $i=1,2,\ldots,n$ and $\ell=1,2,\ldots,s_i$ with s_i being the number of collider points on the i^{th} link.

The position of the collider points $c_{i,\ell}$ is derived from the kinematic transformations T_i^i applied to each link, as

$$\mathbf{c}_{i,\ell} = T_1^i \left[\frac{\ell a_i}{s_i + 1}, 0, 0, 1 \right]^T, \quad \forall \ell \in \{1, 2, \dots, s_i\}$$
 (6)

where $a_i \in \mathbb{R}$ is the length of the i^{th} link.

The set of collider points C_i for the i^{th} link is defined as

$$C_i = \left\{ \mathbf{c}_{i,\ell} \mid \mathbf{c}_{i,\ell} \in \mathbb{R}^3, \forall \ell \in \{1, 2, \dots, s_i\} \right\}$$
 (7)

The complete set of collider points for all links C is

$$C = \bigcup_{i=1}^{n} C_i = \left\{ \mathbf{c}_{i,\ell} \mid \mathbf{c}_{i,\ell} \in \mathbb{R}^3 \, \forall i \in \{1, 2, \dots, n\}, \right.$$
$$\forall \ell \in \{1, 2, \dots, s_i\} \right\}$$
(8)

Each collider point $\mathbf{c}_{i,\ell}$ is located along the body of the robot and moves according to the transformations applied to the i^{th} link of the robot.

D. Valid Robot Trajectories

Let $\mathbf{q}=(\theta_1,\theta_2,\ldots,\theta_n,\alpha_1,\alpha_2,\ldots,\alpha_n,a_1,a_2,\ldots,a_n,d_1,d_2,\ldots,d_n)\in\mathbb{R}^{4n}$ represent the configuration parameters, where $\theta_i\in[0,2\pi)$ and $\alpha_i\in[0,2\pi)$ are the joint angles and link twist angles, respectively, and $a_i\in\mathbb{R}$ and $d_i\in\mathbb{R}$ are the link lengths and offsets, respectively.

To define a set of valid trajectories \mathcal{T}_v for the robot for a workspace W and configuration parameters \mathbf{q} , we consider consecutive neighboring valid actuation values $\mathbf{a}(t)$, ensuring that the norms of the delta distances of the joints' positions in Cartesian space, and joint space, are less than a fixed limit L_{\max} , and there are no collisions between the robot and the obstacles at each time step t.

The set of all actuation values a is defined as

$$\mathbf{a} = \{ (\phi_i(t), \gamma_i(t), \psi_i(t), x_i(t), y_i(t), z_i(t)) \mid t \in [0, 1], \\ \forall i \in \{1, 2, \dots, n\} \}$$
 (9)

where

- $\phi_i(t) \in \mathbb{R}$ represents the rotation about the x-axis (roll).
- $\gamma_i(t) \in \mathbb{R}$ represents the rotation about the y-axis (pitch).
- $\psi_i(t) \in \mathbb{R}$ represents the rotation about the z-axis (yaw).
- $x_i(t) \in \mathbb{R}$ represents the translation along the x-axis.
- $y_i(t) \in \mathbb{R}$ represents the translation along the y-axis.
- $z_i(t) \in \mathbb{R}$ represents the translation along the z-axis for the *i*-th joint at time *t*.

Let $\mathbf{a}_0 = (0,0,\dots,0) \in \mathbb{R}^{6n}$ represent the home position where all actuation values are zero. Let $\mathbf{a}_{\text{task}} \in \mathbb{R}^{6n}$ represent the actuation values that make the end-effector reach the task point. Each trajectory $\mathcal{T}_v(t)$ starts from the home position \mathbf{a}_0 , and ends at the actuation values \mathbf{a}_{task} .

The set of valid trajectories \mathcal{T}_v is defined as

$$\mathcal{T}_{v} = \{\{\mathbf{a}(t) \mid t \in [0,1]\} \mid \mathbf{a}(0) = \mathbf{a}_{0}, \mathbf{a}(1) = \mathbf{a}_{\text{task}}, \tag{10}$$

$$\|f(\mathbf{a}(t + \Delta t)) - f(\mathbf{a}(t))\| + \lambda \|\mathbf{a}(t + \Delta t) - \mathbf{a}(t)\| < L_{\max},$$

$$\mathbf{c}_{i,\ell}(t) - \mathbf{o}_{k}\| > r_{k},$$

$$\forall i \in \{1, 2, \dots, n\}, \forall \ell \in \{1, 2, \dots, s_{i}\},$$

$$\forall t \in [0, 1 - \Delta t], \forall k \in \{1, 2, \dots, m\}\}$$

, where

- $f(\mathbf{a}(t)) \in \mathbb{R}^{3n}$ represents the Cartesian positions of all joints calculated by the forward kinematics function.
- $L_{\text{max}} \in \mathbb{R}$ is the max distance metric between two nodes in each trajectory $\mathbf{a}(\mathbf{t})$ in terms of Cartesian and joint space distances.

• $\|\mathbf{c}_{i,\ell}(t) - \mathbf{o}_k\| > r_k$ ensures that the collider points are outside the obstacles at all times t.

Smaller values of $L_{\rm max}$ ensure smoothness of the robot motion in Cartesian space. Using higher limits is in turn limited by the size of the obstacles and their clearances. If a higher limit $L_{\rm max}$ is applied, there is a potential that some of the obstacles (dependent on their size) could be skipped between a pair of trajectory steps of the robot, and this needs to be accounted for in the kinematic design optimization process.

E. Workspace Reachability

Workspace reachability is defined as the existence of a set of valid robot trajectories \mathcal{T}_v such that all task points in the set \mathcal{P} are reachable by the robot with configuration parameters \mathbf{q} . Formally, the reachability set \mathcal{R} is redefined as a subset of the task points set \mathcal{P} that contains only the points \mathbf{p}_i where a valid trajectory exists

$$\mathcal{R}(\mathbf{q}, W) = \left\{ \mathbf{p}_j \in \mathcal{P} \mid \exists \mathcal{T}_{v_j}(\mathbf{q}) \subset \mathcal{T}_v(\mathbf{q}) : \mathbf{a}(0) = \mathbf{0} \text{ and } \mathbf{a}(1) = \mathbf{a}_{\mathsf{task}, j} \text{ and} \right.$$
$$\mathbf{c}_{\mathsf{end-effector}}(\mathbf{a}_{\mathsf{task}, j}) = \mathbf{p}_j \right\} \tag{11}$$

where

- W is the workspace.
- \mathcal{P} is the set of task points.
- \mathcal{T}_v is the set of valid trajectories.
- $\mathbf{c}_{\text{end-effector}}(\mathbf{a}_{\text{task},j})$ is the position of the end-effector determined by the forward kinematics equation given the actuation values $\mathbf{a}_{\text{task},j}$.

Workspace reachability $R(\mathbf{q},W)$ can be quantified as the ratio between the dimension of the reachability set $\mathcal R$ and the dimension of the task points set $\mathcal P$

$$R(\mathbf{q}, W) = \frac{\dim(\mathcal{R}(\mathbf{q}, W))}{\dim(\mathcal{P})}$$
(12)

III. KINEMATICS OPTIMIZATION FRAMEWORK

In Section II, we formulated a mathematical definition to a generic kinematic design problem of serial robots given tasks and constraints in cluttered environments, via a reduction of a generic kinematic model of the robot. In order to reduce the complexity of the design space, and to increase sampling efficiency of the motion planning aspect of the problem, we further constrain the set of valid trajectories \mathcal{T}_v by imposing trajectory collision constraints to each consecutive configuration of the robot in each valid trajectory.

A. Integrated collision avoidance

The proposed approach examines the space between two successive configurations of the robot from the set of valid trajectories \mathcal{T}_v for collisions with the obstacles defined by the set of obstacles \mathcal{O} .

Let $\mathbf{c}_{i,\ell}(t) = (x_{i,\ell}(t), y_{i,\ell}(t), z_{i,\ell}(t)) \in \mathbb{R}^3$ be the position of the ℓ^{th} collider on the i^{th} link at time t.

We construct a set of line segments \mathcal{L} between the corresponding colliders $\mathbf{c}_{i,\ell}(t)$ at two consecutive time steps,

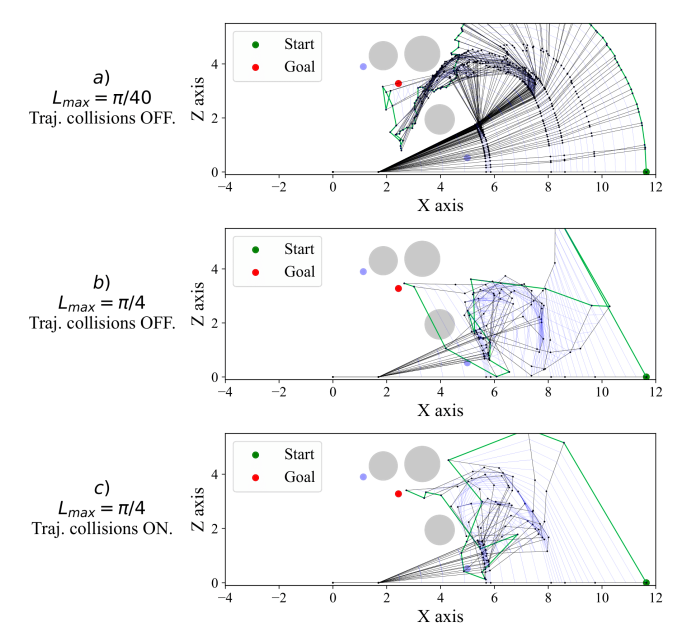


Fig. 1: Visualisation of the effects of the proposed integrated trajectory collision detection for path planning. In cases such as b), a collision is not detected and the robot can move over the obstacle due to the coarser sampling of the joint space $(L_{\rm max}=\pi/4)$. The proposed trajectory collision checking c), successfuly avoids all obstacles for $(L_{\rm max}=\pi/4)$. The proposed trajectory collision lines are shown in blue.

t and $t + \Delta t$, and then check if any of these line segments intersect with any of the obstacles from \mathcal{O} .

The set of collision mesh lines \mathcal{L} is defined as:

$$\mathcal{L} = \left\{ (\mathbf{c}_{i,\ell}(t), \mathbf{c}_{i,\ell}(t + \Delta t)) \mid \mathbf{c}_{i,\ell}(t) \in \mathbb{R}^3 \right.$$

$$\forall i \in \{1, 2, \dots, n\}, \forall \ell \in \{1, 2, \dots, s_i\}, \forall t \in [0, 1 - \Delta t] \right\}$$

where

- $\mathbf{c}_{i,\ell}(t)$ is the position of the ℓ^{th} collider on the i^{th} link at time t.
- $\mathbf{c}_{i,\ell}(t+\Delta t)$ is the position of the ℓ^{th} collider on the i^{th} link at time $t+\Delta t$.

The collision condition for a line segment and a spherical obstacle can be defined based on the minimum distance between the line segment and the center of the sphere. The minimum distance between a line segment $(\mathbf{c}_1, \mathbf{c}_2)$ and a point \mathbf{o} is given by

$$d_{\min} = \frac{\|(\mathbf{c}_2 - \mathbf{c}_1) \times (\mathbf{c}_1 - \mathbf{o})\|}{\|\mathbf{c}_2 - \mathbf{c}_1\|}$$
(14)

where \times denotes the cross product and $\|\cdot\|$ denotes the Euclidean norm. For a valid line segment, where there are no collision conditions active, the minimum distance d_{\min} should be greater than the sum of the obstacle radius r_k and a clearance ϵ

$$d_{\min} > r_k + \epsilon \tag{15}$$

Thus, the set of valid line segments \mathcal{L}_{valid} is defined as

$$\mathcal{L}_{\text{valid}} = \left\{ (\mathbf{c}_{i,\ell}(t), \mathbf{c}_{i,\ell}(t + \Delta t)) \mid \mathbf{c}_{i,\ell}(t) \in \mathbb{R}^{3} \right.$$

$$\forall i \in \{1, 2, \dots, n\}, \forall \ell \in \{1, 2, \dots, s_{i}\},$$

$$\forall t \in [0, 1 - \Delta t], \forall k \in \{1, 2, \dots, m\},$$

$$\frac{\|(\mathbf{c}_{i,\ell}(t + \Delta t) - \mathbf{c}_{i,\ell}(t)) \times (\mathbf{c}_{i,\ell}(t) - \mathbf{o}_{k})\|}{\|\mathbf{c}_{i,\ell}(t + \Delta t) - \mathbf{c}_{i,\ell}(t)\|} > r_{k} + \epsilon \right\}$$

where

- $\mathbf{c}_{i,\ell}(t)$ is the position of the ℓ^{th} collider on the i^{th} link at time t.
- $\mathbf{c}_{i,\ell}(t+\Delta t)$ is the position of the ℓ^{th} collider on the i^{th} link at time $t+\Delta t$.
- $\mathbf{o}_k \in \mathbb{R}^3$ is the center of the k^{th} obstacle.
- $r_k \in \mathbb{R}$ is the radius of the k^{th} obstacle.
- $\epsilon \in \mathbb{R}$ is the clearance.

Now we can further constrain the set of valid trajectories \mathcal{T}_v and redefine it as follows:

$$\mathcal{T}_{v} = \{\{\mathbf{a}(t) \mid t \in [0, 1]\} \mid \mathbf{a}(0) = \mathbf{a}_{0}, \mathbf{a}(1) = \mathbf{a}_{task}, \\ \|f(\mathbf{a}(t + \Delta t)) - f(\mathbf{a}(t))\| + \lambda \|\mathbf{a}(t + \Delta t) - \mathbf{a}(t)\| < L_{max}, \\ \|\mathbf{c}_{i,\ell}(t) - \mathbf{o}_{k}\| > r_{k} + \epsilon, \\ \forall i \in \{1, 2, \dots, n\}, \forall \ell \in \{1, 2, \dots, s_{i}\}, \\ \forall t \in [0, 1 - \Delta t], \forall k \in \{1, 2, \dots, m\}, \\ \dim(\mathcal{L}_{v}) = \dim(\mathcal{L})\}$$

$$(17)$$

where

- $\mathbf{a}(t) \in \mathbb{R}^{6n}$ represents the actuation parameters at t.
- $f(\mathbf{a}(t)) \in \mathbb{R}^{3n}$ represents the Cartesian positions of all joints calculated by the forward kinematics function.
- $L_{\max} \in \mathbb{R}$ is the fixed limit for the delta distances.
- a₀ represents the home position.
- a_{task} represents the actuation values reaching the task point.
- $\|\mathbf{c}_{i,\ell}(t) \mathbf{o}_k\| > r_k + \epsilon$ ensures that the collider points are outside the obstacles at all times t.
- $\dim(\mathcal{L}_v)$ is the dimension of the set of valid line segments that are not colliding with obstacles.
- $\dim(\mathcal{L})$ is the dimension of the original set of line segments.

By iterating through all colliders and time steps along the trajectory, and ensuring that all line segments satisfy the collision condition, the proposed method ensures that the robot's path is collision-free.

B. Optimization via a Kinematic Design Synthesis

This study aims to achieve a collective kinematic design synthesis by means of optimizing the lengths and number of links, but also ranges, number, type of actuators, as defined in the proposed generic form of the kinematic model of a serial robot in Section II-A. Here, we introduce constraints on the upper and lower bounds of the joint axes (Tait–Bryan angles and translations) and use them as additional design variables to enable optimization of the number and type of

DOFs of the proposed generic robot model. The upper and lower bounds for the joint axes are defined as follows

$$\phi_i^{\min} \le \phi_i \le \phi_i^{\max}, \qquad \gamma_i^{\min} \le \gamma_i \le \gamma_i^{\max},
\psi_i^{\min} \le \psi_i \le \psi_i^{\max}, \qquad \mathbf{x}_i^{\min} \le x_i \le \mathbf{x}_i^{\max},
\mathbf{y}_i^{\min} \le y_i \le \mathbf{y}_i^{\max}, \qquad \mathbf{z}_i^{\min} \le z_i \le \mathbf{z}_i^{\max}$$
(18)

Let the vectors of lower and upper bounds for each joint axis for each link i, and DH parameters of each link be

$$\mathbf{q}_i = (\theta_i, \alpha_i, a_i, d_i) \in \mathbb{R}^4 \tag{19}$$

$$\mathbf{a}_{i}^{\min} = (\boldsymbol{\phi}_{i}^{\min}, \boldsymbol{\gamma}_{i}^{\min}, \boldsymbol{\psi}_{i}^{\min}, \mathbf{x}_{i}^{\min}, \mathbf{y}_{i}^{\min}, \mathbf{z}_{i}^{\min}) \in \mathbb{R}^{6}$$
 (20)

$$\mathbf{a}_{i}^{\text{max}} = (\phi_{i}^{\text{max}}, \gamma_{i}^{\text{max}}, \psi_{i}^{\text{max}}, \mathbf{x}_{i}^{\text{max}}, \mathbf{y}_{i}^{\text{max}}, \mathbf{z}_{i}^{\text{max}}) \in \mathbb{R}^{6}$$
 (21)

The combined design space for all links can be given as

$$\mathbf{x} = (\mathbf{q}_1, \dots, \mathbf{q}_n, \mathbf{a}_1^{\min}, \dots, \mathbf{a}_n^{\min}, \mathbf{a}_n^{\max}, \dots, \mathbf{a}_n^{\max}) \in \mathbb{R}^{16n}$$
(22)

The proposed optimization problem aims to find the optimal set of robot parameters q, and joint axis bounds amin and amax that maximize the workspace reachability $R(\mathbf{q}, W, \mathbf{a}^{\min}, \mathbf{a}^{\max})$, ensuring that all task points in the workspace are reachable, while minimizing the arctan of the total link lengths and joint axis ranges. Formally, the optimization problem is defined as follows

$$\min_{\mathbf{x}} \quad \lambda_0 (1 - R(\mathbf{x}(\mathbf{q}, \mathbf{a}^{\min}, \mathbf{a}^{\max}), W)) \qquad (23)$$

$$+ \sum_{i=1}^{n} (\lambda_1 A_i + \lambda_2 B_i + \lambda_3 C_i + \lambda_4 D_i) + \lambda_5 E$$

subject to $\mathbf{q}_i \in \mathbb{R}^4$ and $\mathbf{q}_i^{\min} \leq \mathbf{q}_i \leq \mathbf{q}_i^{\max}$ (24)

$$\mathbf{a}_{i}^{\text{initial min}} \le \mathbf{a}_{i}^{\min} \le \mathbf{a}_{i}^{\max} \le \mathbf{a}_{i}^{\text{initial max}},$$
 (25)

$$\begin{cases}
A_{i} = \arctan(a_{i}) & \text{if } R = 1 \\
A_{i} = 1 & \text{if } R < 1
\end{cases}$$

$$\begin{cases}
B_{i} = \arctan(\mathbf{a}_{i}^{\max} - \mathbf{a}_{i}^{\min}) & \text{if } R = 1 \\
B_{i} = 1 & \text{if } R < 1
\end{cases}$$

$$\begin{cases}
C_{i} = 1 & \text{if } a_{i} > 0 \\
C_{i} = 0 & \text{if } a_{i} = 0
\end{cases}$$
(28)

$$\begin{cases} B_i = \arctan(\mathbf{a}_i^{\text{max}} - \mathbf{a}_i^{\text{min}}) & \text{if } R = 1\\ B_i = 1 & \text{if } R < 1 \end{cases}, \tag{27}$$

$$\begin{cases}
C_i = 1 & \text{if } a_i > 0 \\
C_i = 0 & \text{if } a_i = 0
\end{cases}$$
(28)

$$\begin{cases}
D_i = 1 & \text{if } \mathbf{a}_i^{\text{max}} - \mathbf{a}_i^{\text{min}} > 0 \\
D_i = 0 & \text{if } \mathbf{a}_i^{\text{max}} - \mathbf{a}_i^{\text{min}} = 0
\end{cases}$$
(29)

$$\begin{cases}
E = 0 & \text{if } R = 1 \\
E = 1 & \text{if } R < 1
\end{cases}$$
(30)

$$\forall i \in \{1, 2, \dots, n\} \tag{31}$$

where

- $R(\mathbf{x}(\mathbf{q}, \mathbf{a}^{\min}, \mathbf{a}^{\max}), W)$ is the reachability ratio for a given configuration q, workspace W, and joint axis bounds \mathbf{a}_{i}^{\min} and \mathbf{a}_{i}^{\max} .
- $\lambda_{1...5}$ is a weighting factor used to balance the objec-
- $\arctan(\mathbf{a}_i^{\max} \mathbf{a}_i^{\min})$ denotes the sum of the arctangent of the joint axis ranges values.
- a^{initial max} is the initial upper bound for the joint axes.
- a^{initial min} is the initial lower bound for the joint axes.

IV. RESULTS

The results were evaluated based on the time efficiency of the kinematic design optimization for reachability of targets. The optimal design framework is not constrained to a specific method for solving the optimization problem proposed in Section III-B. Therefore, in order to determine the most appropriate optimization method to use forward, a comparative analysis was performed between ASA used in [11], Particle Swarm Optimization (PSO) [15], and Genetic Algorithm (GA) [16], as common benchmarks in the literature. We compare the baseline method (ASA+RRT) [11] which does not use the proposed trajectory collision detection, to other sampling methods (ASA, PSA, GA) all which are set to use the proposed trajectory collision detection (Section II-A) integrated in the RRT motion planning step. For the baseline method (ASA+RRT) [11], the maximum distance between the nodes in the trajectories of the motion planning method (RRT) was set to $L_{\rm max}=\pi/40$. This value was experimentally tuned to the maximum value for which the robot will not move over obstacle, and is depended on the size of the smallest obstacle in the environment as illustrated in Fig. 1. For the rest of the sampling methods, the maximum distance between the nodes in the trajectories of the motion planning method (RRT) was set to $L_{\text{max}} = \pi/4$, allowing larger distance between samples of robot configuration.

A. Comparative analysis for rate of convergence in a planar workspace.

The analysis was performed in a simplified 2D (XZ)workspace $W = \mathcal{O}_i \cup \mathcal{P}_j, \forall i \in 1, 2, ..., 5, \forall j \in 1, 2, ..., 10.$ The design variables used in this case are $x = q_p$, where $\mathbf{q_p} = (a_1, a_2, \dots, a_8) \in \mathbb{R}^{1 \times 8}$ are the lengths of each link and n = 8 is the size of the kinematic parametric model Eq. (1). The subset of the actuation variables used in this analysis are $\mathbf{a}_{\mathbf{p}} = (\gamma_1, \gamma_2, \dots, \gamma_8) \in \mathbb{R}^{1 \times 8}$, where each actuator performed rotation solely along the y axis. The rest of the actuation variables set to zero.

This experiment was implemented in Python, utilizing the generic versions of ASA, PSO, GA, and RRT algorithms, and was executed on an Intel i9 laptop with 32GB RAM, with the parameters tuned manually. Ten optimization runs were conducted, each with a unique randomized workspace

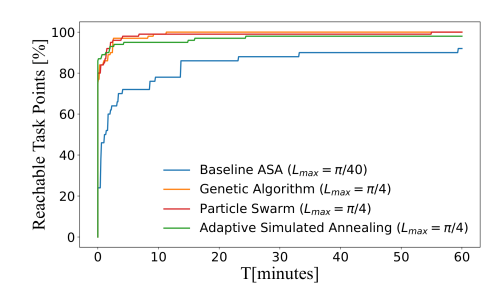


Fig. 2: Optimisation performance for workspace reachability using ASA, PSO, GA with trajectory collision checking and max node-to-node distance $L_{\text{max}} = \pi/4$, and ASA without improved trajectory collision checking and $L_{\text{max}} = \pi/40$.

W and design vector \mathbf{x} . Each run was constrained to 60 minutes, resulting in averaged reachability as Fig. 2 shows.

The results shown in Fig. 2 indicate that the combination of GA and RRT, with the proposed trajectory collision constraints and $L_{\rm max}=\pi/4$, outperformed both PSO and ASA, under similar conditions, and significantly outperformed the baseline ASA + RRT approach [11] in terms of the rate of their convergence. Therefore, GA is used in the evaluation of the convergence rate in the next experiment.

B. Kinematic design synthesis in a volumetric workspace

The proposed design framework is evaluated for reachability of targets in a 3D setting where both link lengths and DOFs are optimised simultaneously in order to prove its rate of convergence. A workspace W was defined with 32 spherical obstacles and 10 task points: $W = \mathcal{O}_i \cup \mathcal{P}_j, \forall i \in 1,2,...,32, \forall j \in 1,2,...,10$. The size of the parametric kinematic model of the robot Eq. (1), is the same as in the 2D experiment and it is set to n=8.

The robot configuration was set to includes one prismatic joint on the x axis per link, followed by two rotational joints ϕ and γ on the x and y axes. The remaining actuation variables were set to zero.

Therefore, the actuation subset was defined as $\mathbf{a_p} = (\phi_1, \phi_2, \dots, \phi_8, \gamma_1, \gamma_2, \dots, \gamma_8, x_1, x_2, \dots, x_8) \in \mathbb{R}^{3 \times 8}$, with the design space vector extended to $\mathbf{x} = \mathbf{q_p}, \mathbf{a_p^{min}}, \mathbf{a_p^{max}} \in \mathbb{R}^{7 \times 8}$. Here, $\mathbf{a_p^{min}}$ and $\mathbf{a_p^{max}}$ represent the minimum and maximum ranges for ϕ , γ , and x.

An experiment was conducted using a randomized workspace W and initial conditions $\mathbf{q_p}$, $\mathbf{a_p^{min}}$, and $\mathbf{a_p^{max}}$, forming the design vector \mathbf{x} . Ten runs were performed to ensure consistency with the results averaged.

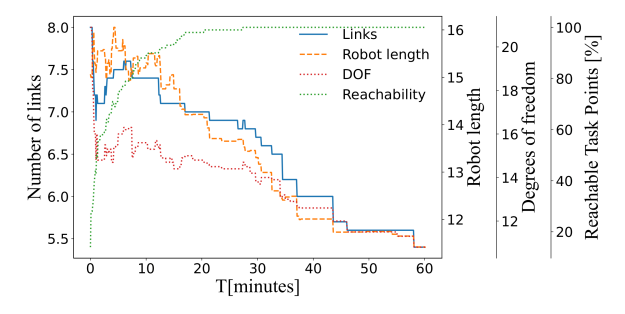


Fig. 3: Average results for simultaneous dimension and type synthesis of a serial robot for workspace reachability in 3D case, achieved over 10 experimental runs with randomized start conditions q_p and workspace W.

The results shown on Fig. 3, demonstrate the convergence rate of the proposed optimization framework for simultaneous kinematic design and type synthesis of serial robots for workspace reachability. The framework effectively optimises the length and number of links, and range, number, and type of DOFs, all while achieving 100% target reachability. Compared to the results in the 2D setting case (Fig. 2), the convergence rate of the reachable targets is expectantly lower due to increased complexity of the problem (3D), and the higher number of design variables used.

V. DISCUSSION

Designing cost-effective bespoke robotic systems in cluttered settings depends on time efficient kinematic design of manipulators (regardless of its DOFs) given space constraints, and design constraints (e.g., minimum link length) for achieving tasks specific to the application of the robot.

The combination of GA for sampling in design space, and RRT with the proposed integrated trajectory collision detection for sampling in configuration space, provides robust rate of convergence, with a significant improvement over the state of the art [11] in a 2D case, and prove the timely convergence of the approach for simultaneous optimization of length and number of links, and number and type of DOFs for attaining 100% of target reachability in a complex 3D cluttered case.

The proposed trajectory collision detection (Section III-A), assumes linear interpolation between the Cartesian paths of the robot's collision points. While this works well for intermediate angle/length displacements of the robot joints, we recommend that a limit to the upper bound of $L_{\rm max}$ is used (e.g. $\pi/3$) to attain this assumption. This issue can be mitigated by increasing the clearance between obstacles and the robot during collision checks.

Our results use a scheduler that starts with a larger value of $L_{\rm max}$ to enable rapid coarse exploration of the workspace, gradually reducing $L_{\rm max}$ to improve motion planning in tighter spaces. Another scheduler increases the maximum iterations for RRT as the high-level optimizer converges, facilitating better workspace exploration as design variables approach optimal values [11].

While RRT does not provide optimal trajectories, it effectively addresses workspace reachability, which is the focus and one key contribution of this study. The supreme convergence properties demonstrates the applicability of our approach for a wide range of real-world scenarios, from space to medical robotics, where customized solutions are essential. While the results are promising, future research could explore dynamic models with constraints like mass, torque, and payload capacity. Integrating advanced machine learning algorithms could further improve efficiency and adaptability.

VI. CONCLUSION

By integrating enhanced motion planning through trajectory collision detection into the design process, the proposed design framework significantly increased the convergence rate of kinematic design optimization in cluttered environments. The combination of the proposed motion planning for reachability estimation, paired with Genetic Algorithm for iteration of design variables, has proven effective in optimizing both the structure and dimensions of serial robots via the kinematic design synthesis, ensuring maximum reachability in various cluttered environments in 3D. This research provided a tool that is intended to be used by design engineers, from the medical, nuclear or space sectors, to mitigate design uncertainty at early stages in order to prevent critical implications to budget, safety and schedule.

REFERENCES

- A. Morgan, J. Abdi, M. Syed, G. Kohen, P. Barlow, and M. Vizcaychipi, "Robots in Healthcare: a Scoping Review," *Current Robotics Reports*, vol. 3, Oct. 2022.
- [2] R. Smith, E. Cucco, and C. Fairbairn, "Robotic Development for the Nuclear Environment: Challenges and Strategy," *Robotics*, vol. 9, p. 94, Dec. 2020. Number: 4 Publisher: Multidisciplinary Digital Publishing Institute.
- [3] A. Flores-Abad, O. Ma, K. Pham, and S. Ulrich, "A review of space robotics technologies for on-orbit servicing," *Progress in aerospace* sciences, vol. 68, pp. 1–26, 2014.
- [4] J. R. R. A. Martins and A. Ning, Engineering Design Optimization. Cambridge University Press, 1 ed., Nov. 2021.
- [5] C. Paredis and P. Khosla, "An approach for mapping kinematic task specifications into a manipulator design," in *Fifth International Con*ference on Advanced Robotics 'Robots in Unstructured Environments, pp. 556–561 vol.1, June 1991.
- [6] J.-O. Kim and P. Khosla, "A formulation for task based design of robot manipulators," in *Proceedings of 1993 IEEE/RSJ International Conference on Intelligent Robots and Systems (IROS '93)*, vol. 3, pp. 2310–2317 vol.3, July 1993.
- [7] S. Patel and T. Sobh, "Task based synthesis of serial manipulators," Journal of Advanced Research, vol. 6, pp. 479–492, May 2015.
- [8] T. Kivelä, J. Mattila, and J. Puura, "A generic method to optimize a redundant serial robotic manipulator's structure," *Automation in Construction*, vol. 81, pp. 172–179, Sept. 2017.
- [9] O. W. Maaroof, M. I. C. Dede, and L. Aydin, "A Robot Arm Design Optimization Method by Using a Kinematic Redundancy Resolution Technique," *Robotics*, vol. 11, p. 1, Dec. 2021.
- [10] J. Burgner-Kahrs, H. Gilbert, and R. III, "On the Computational Design of Concentric Tube Robots: Incorporating Volume-Based Objectives," in 2013 IEEE International Conference on Robotics and Automation, May 2013.
- [11] C. Baykal, C. Bowen, and R. Alterovitz, "Asymptotically Optimal Kinematic Design of Robots using Motion Planning," *Autonomous robots*, vol. 43, pp. 345–357, Feb. 2019.
- [12] L. Ingber, "Adaptive simulated annealing (asa): Lessons learned," Control Cybernetics, vol. 25, pp. 33–54, 01 1996.
- [13] H. Gamper, A. Luthi, H. Gattringer, A. Mueller, and M. Di Castro, "Kinematic Model Pruning: A Design Optimization Technique for Simultaneous Optimization of Topology and Geometry," *Robotics*, vol. 11, p. 31, Apr. 2022. Number: 2 Publisher: Multidisciplinary Digital Publishing Institute.
- [14] M. W. Spong and M. Vidyasagar, Robot Dynamics and Control. New York: John Wiley and Sons, 1989.
- [15] J. Kennedy and R. Eberhart, "Particle swarm optimization," in *Proceedings of ICNN'95 International Conference on Neural Networks*, vol. 4, pp. 1942–1948 vol.4, Nov. 1995.
- [16] J. H. Holland, Adaptation in Natural and Artificial Systems. Ann Arbor, MI: University of Michigan Press, 1975. second edition, 1992.